Search for Ultra High Energy Primary Photons at the Pierre Auger Observatory

Roberta Colalillo
for The Pierre Auger Collaboration

Federico II University and INFN of Naples, Italy

10/01/2014, RICAP-14, Noto (Sicily, Italy)

The Pierre Auger Observatory Energy Range

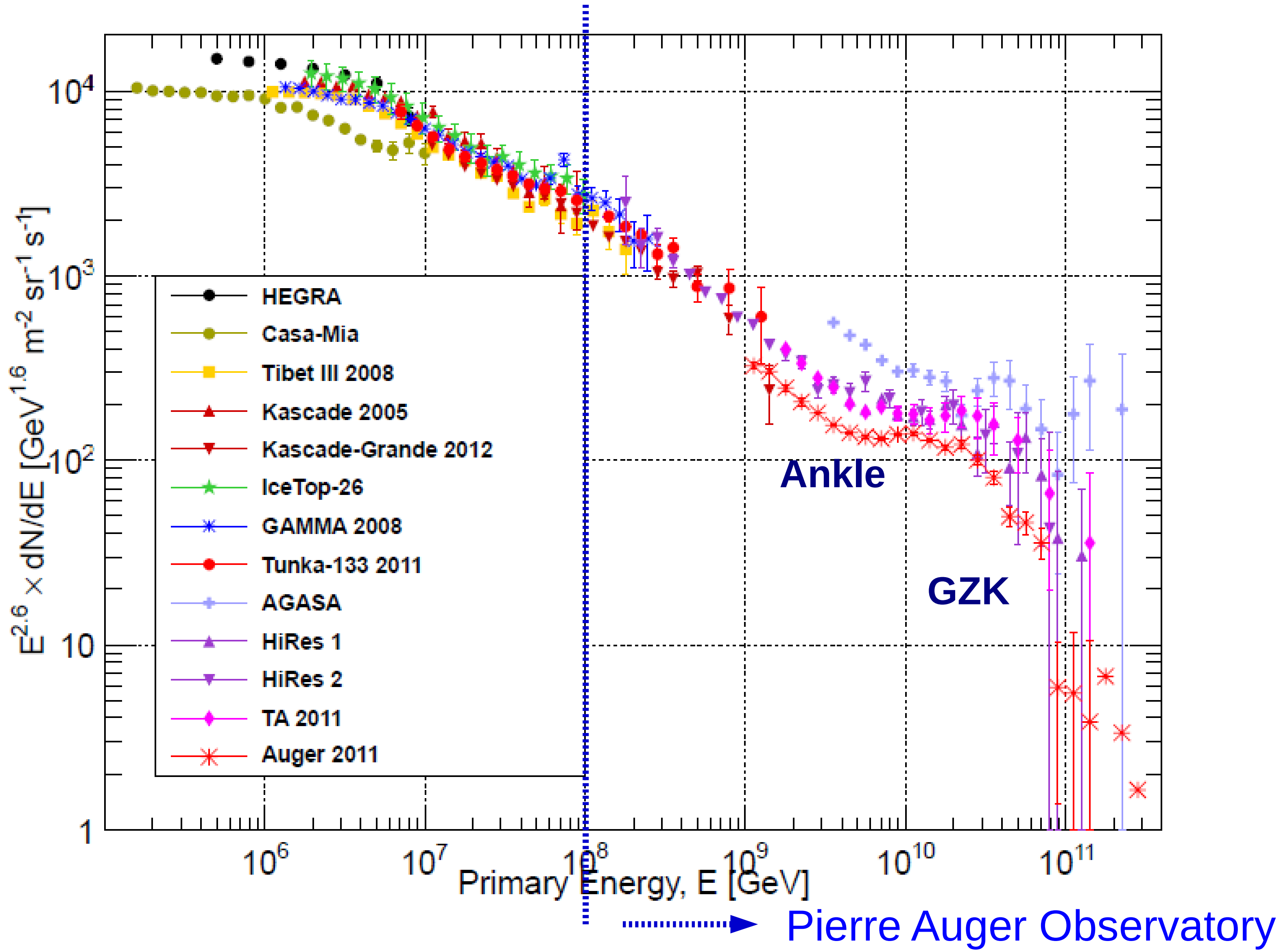

Open Questions

In the energy range of interest for the Pierre Auger Observatory, two structures are visible in the cosmic ray spectrum:

<u>Ankle:</u> it could represent the transition from a Galactic powerlaw behavior to an extragalactic contribution or could be a “dip” due to $e^{\pm}$ pair production in a cosmic-ray spectrum that is dominated by protons of extragalactic origin.

<u>Cutoff at $4x10^{19}$eV:</u> it could be related to the <u>GZK effect</u> or to the maximum energy reached by the acceleration sources (“<u>bottom-up</u>” models).

The search of UHE photons
can help to solve these misteries

Possible sources of UHE photons are:
- GZK process;
- the production by nuclei in regions of intense star light;
- “top-down” models (decay of exotic particles directly at the energies observed)

GZK process

The GZK cutoff is related to the interaction of cosmic ray primaries with the CMB (Cosmic Microwave Background) :

$$p + \gamma_{2.7K} \rightarrow \begin{cases} \pi^0 + p \\ \pi^+ + n \\ p + e^+ + e^- \end{cases}$$

$$A + \gamma_{2.7K} \rightarrow \begin{cases} (A-1) + N \\ (A-2) + 2N \\ A + e^+ + e^- \end{cases}$$

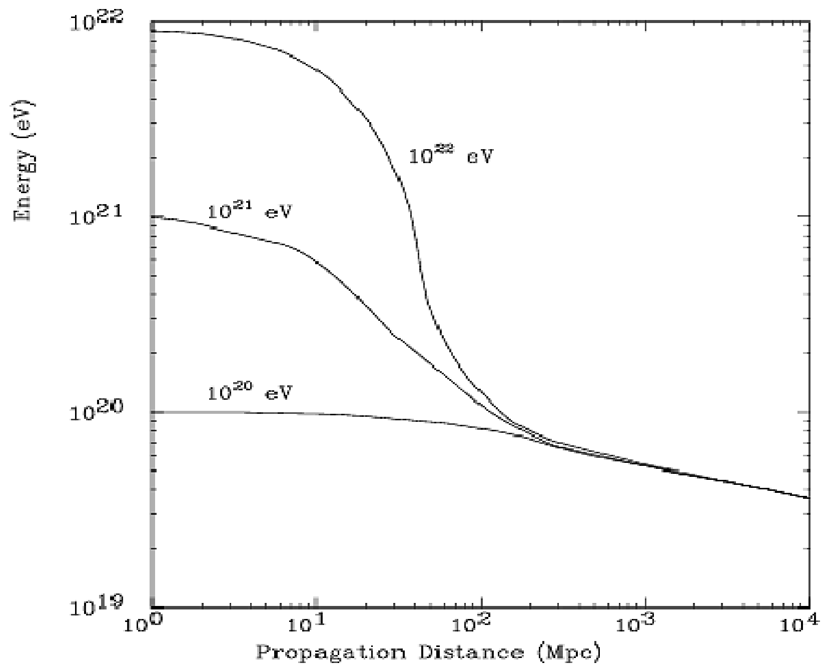

GZK photons come from the π^0 decay and are typically a factor ~10 below the primary nucleon energy.

- Photons interact with EBR (Extragalactic Background Radiation) via e^+e^- production
- Electrons via Inverse Compton Scattering (ICS)

Motivations of UHE photon search

- Search for GZK photons, to prove the GZK effect and constrain source and propagation models;
- Search for astronomical sources;
- Study the impact on the measurements of energy spectrum, cross sections, mass composition and possible consequences for fundamental physics
- Set significant limits to the possible contribution of top-down mechanisms to the primary cosmic-ray flux;

Three analysis:

1. diffuse upper limit with the surface detector data;
2. diffuse upper limit with the hybrid data;
3. directional upper limit with the hybrid data;

UHE photon showers

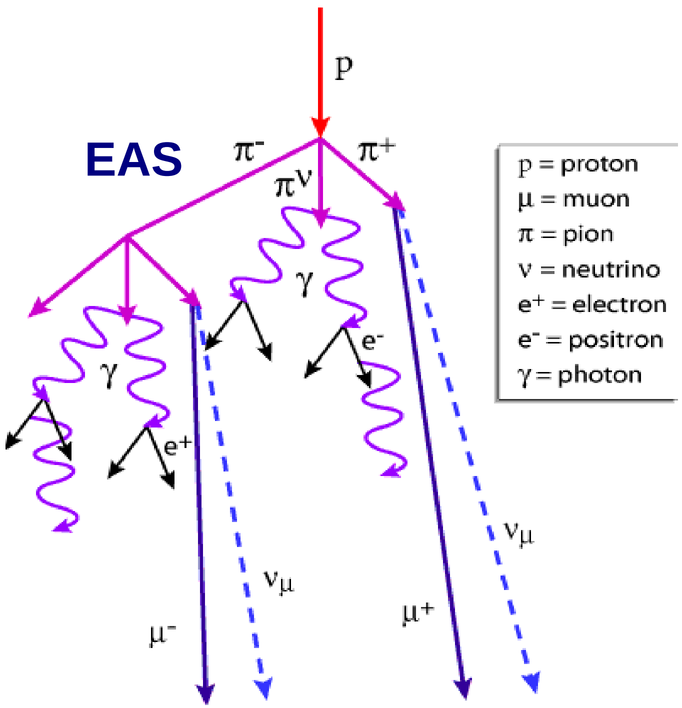

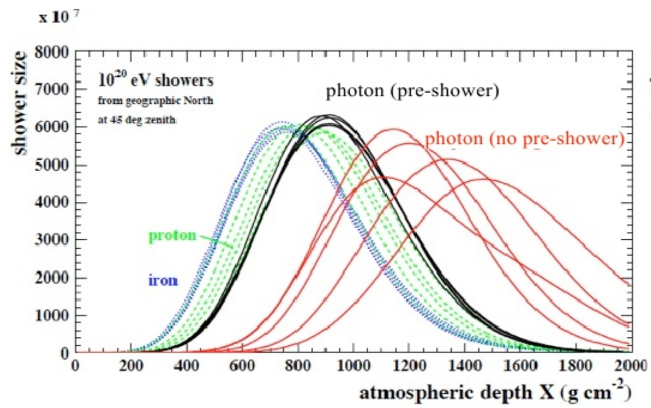

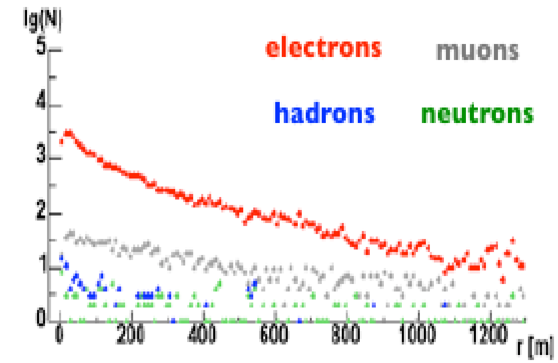

http://www-ik.fzk.de/corsika/

Photon-initiated cascades are almost purely electromagnetic → **smaller muon content**

σ_{BH} ($\gamma \rightarrow e+e-$)<$\sigma_{hadronic}$ → **deeper shower (larger Xmax)**

Other variables, related to X_{max} or N_μ or a combination of both, have a good discriminating power

Xmax

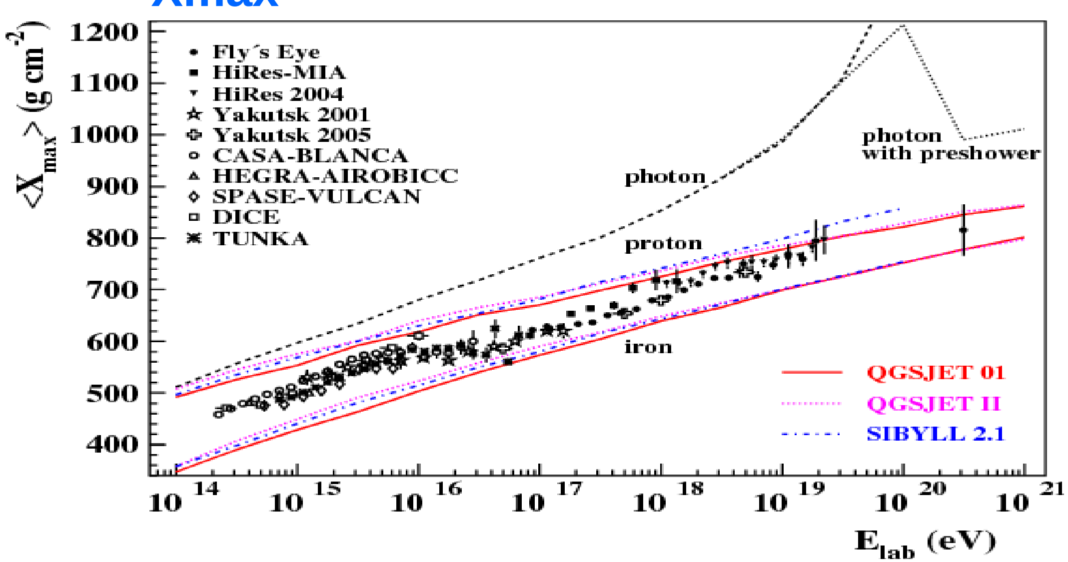

Muon Content

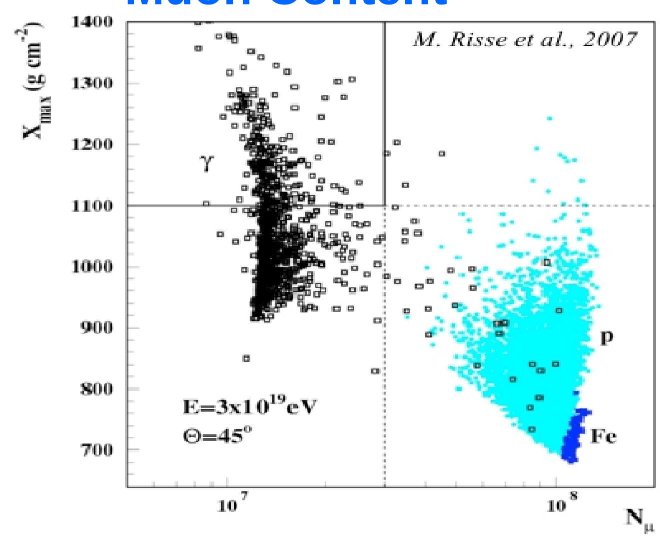

The Pierre Auger Observatory

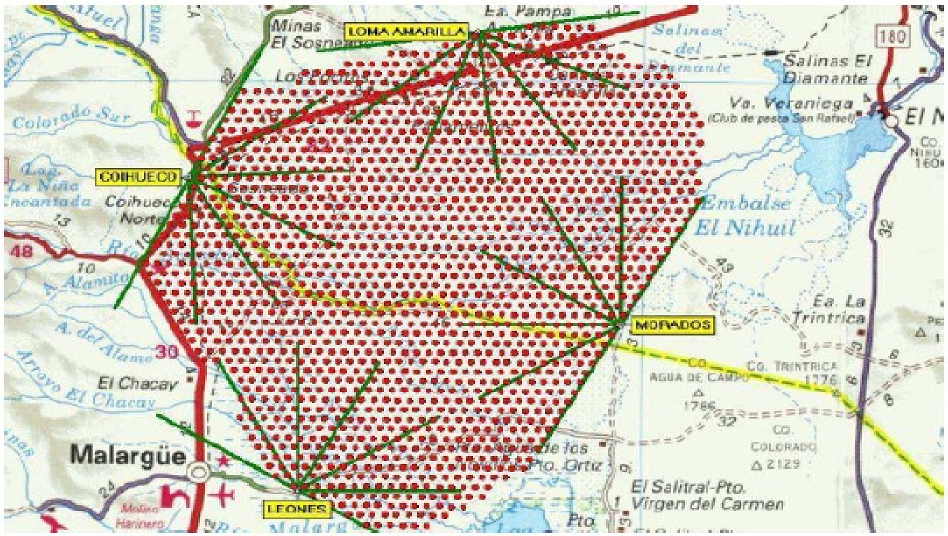

Goal of the Experiment:

- Energy Spectrum;
- Mass Composition;
- Arrival Directions - Anisotropy

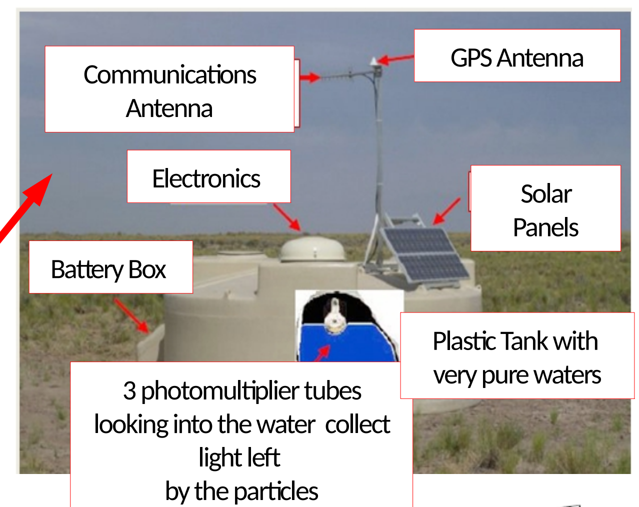

100% duty cycle, but energy estimation related to hadronic models

SD detector: 1600 Water Cherenkov detectors, covering 3000 km^2 and arranged in a triangular grid with 1500 m spacing.
FD detector: 24 telescopes, 6 for each sites that are on the perimeter of the surface array.
The site is located in the Argentinian pampas, at 1400 m above sea level (880 g/cm2).

- **Large Aperture**
- **Hybrid Detection Technique**

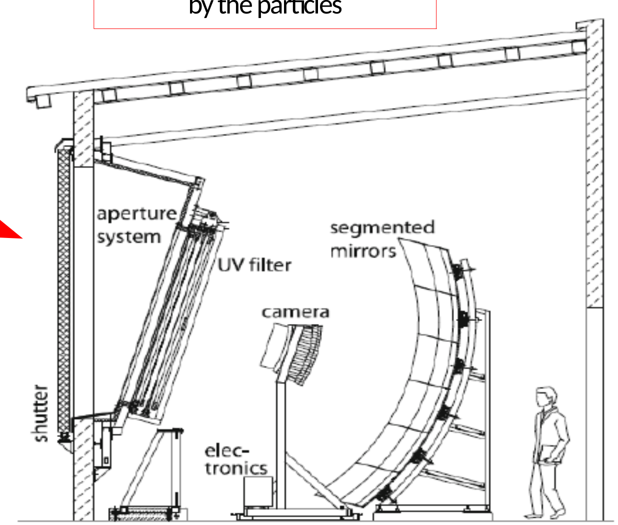

calorimetric energy, but 10% duty cycle

The Hybrid Reconstruction

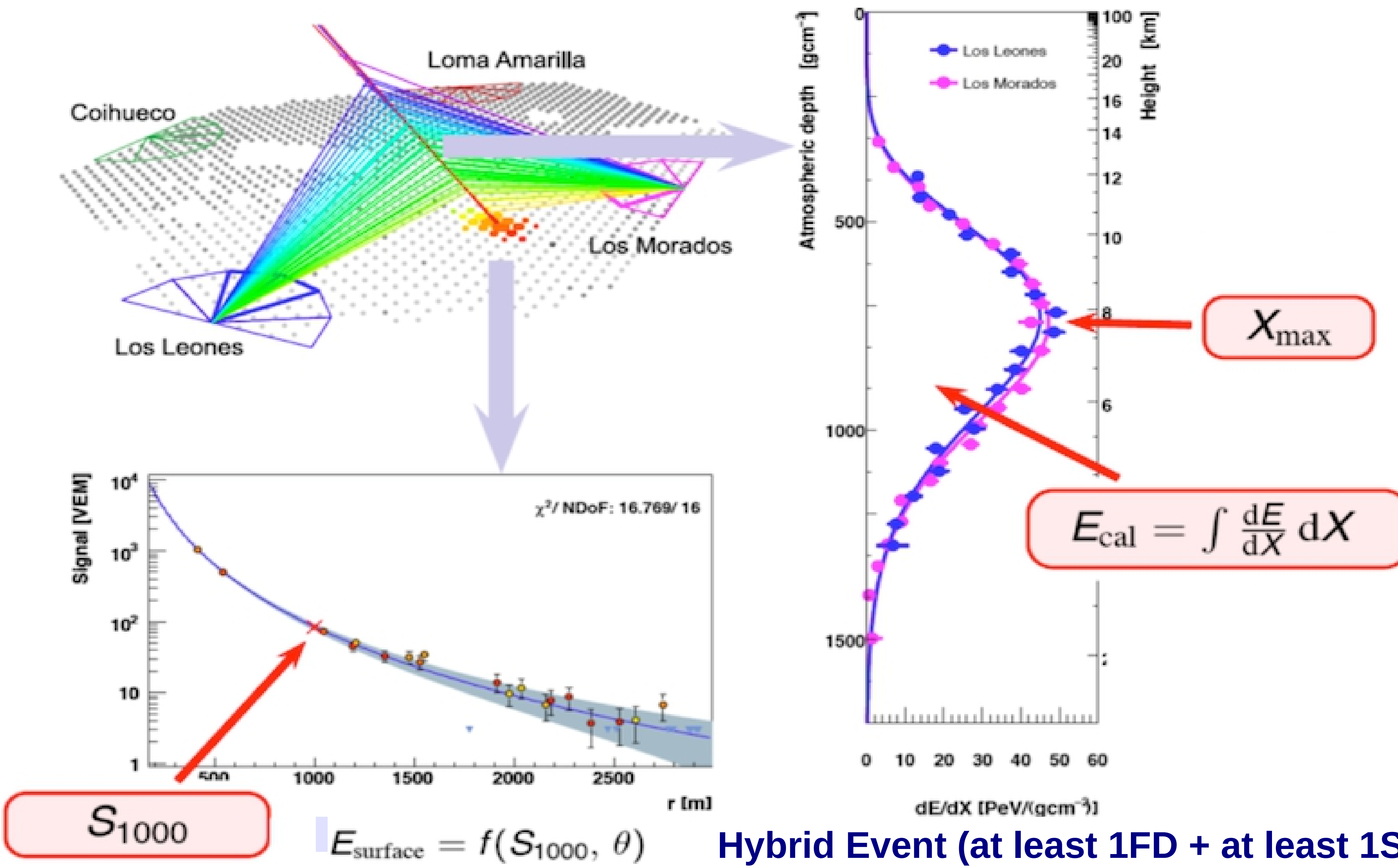

Hybrid Event (at least 1FD + at least 1SD):

- accurate energy and direction measurements;
- complementary mass sensitive parameters;
- calibration of the energy scale for SD events and extension to lower energies

Upper Limit using SD

Using data taken by the Auger surface detector in the period 1 January 2004 to 31 December 2006, a **limit on the flux and on the fraction of photons** were derived.
The upper limits are calculated for data with energy
above 10^{19}eV, 2 x 10^{19}eV, 4 x 10^{19}eV and **primary zenith angles of 30°–60°**

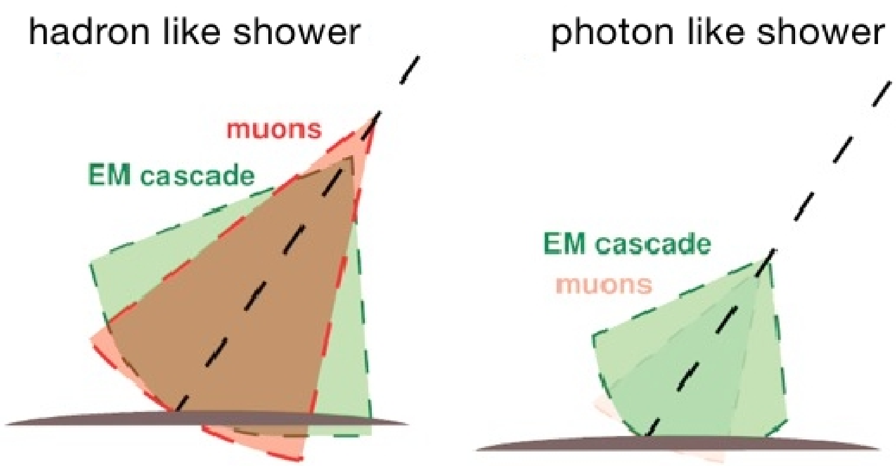

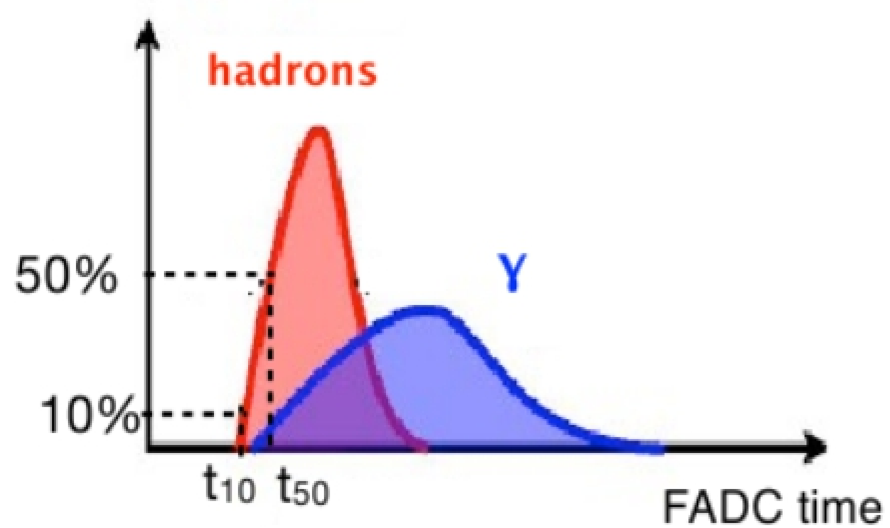

Radius of Curvature: R

Risetime: $t_{1/2} = t_{50\%} - t_{10\%}$

Smaller radius of curvature for photon-initiated showers → geometric reasons and muon content

Larger risetime of the signal for deeper showers → less muons and larger geometric spread of the particle arriving time to the station

Deviation Δ_X

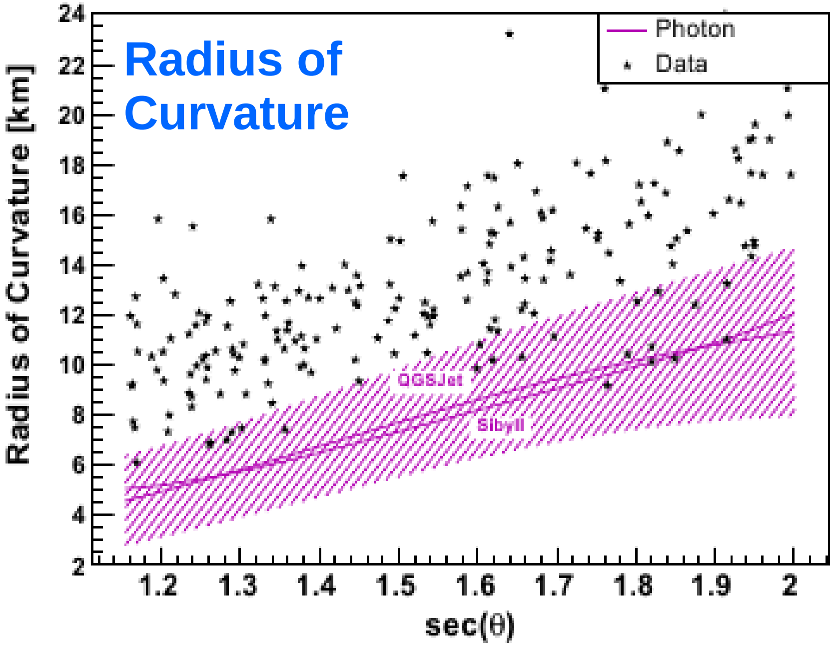

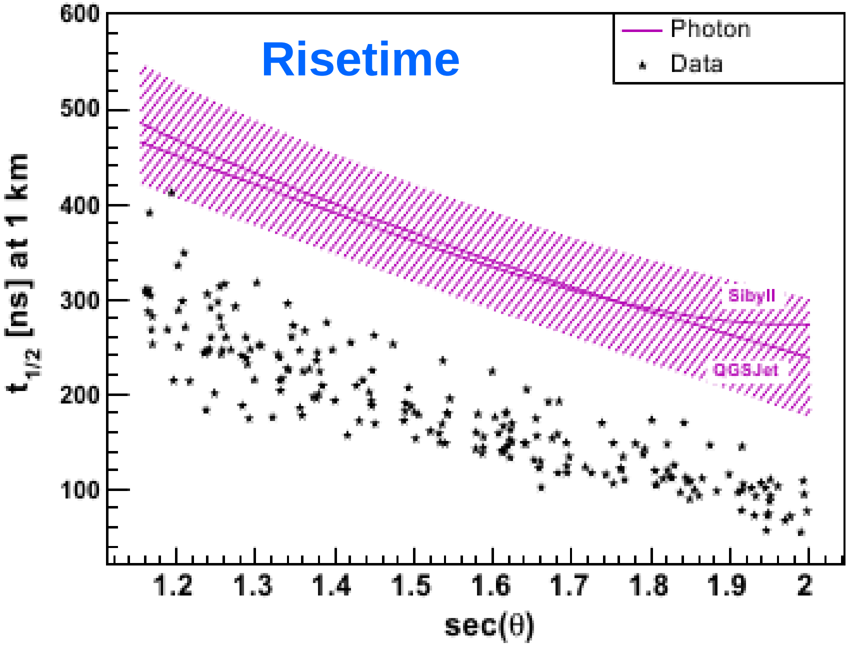

$$\Delta_x = \frac{x - \bar{x}_\gamma(S(1000), \theta)}{\sigma_{x,\gamma}(S(1000), \theta)}$$

$x = t_{1/2}$ or $x = R$

x_γ and $\sigma_{x,\gamma}$ are the mean value and the spread obtained from simulated primary photons

The Discriminant Method

Principal Component Analysis

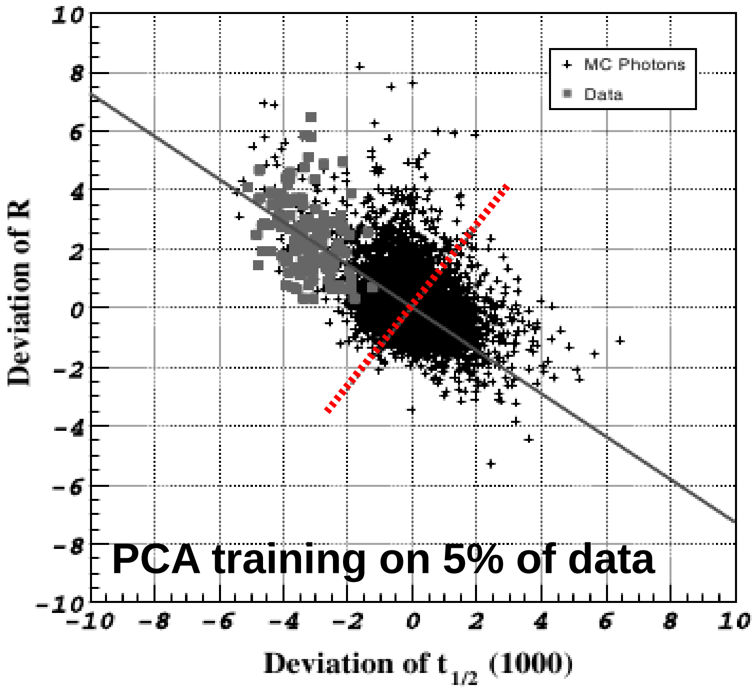

The median of photon
distribution chosen as cut

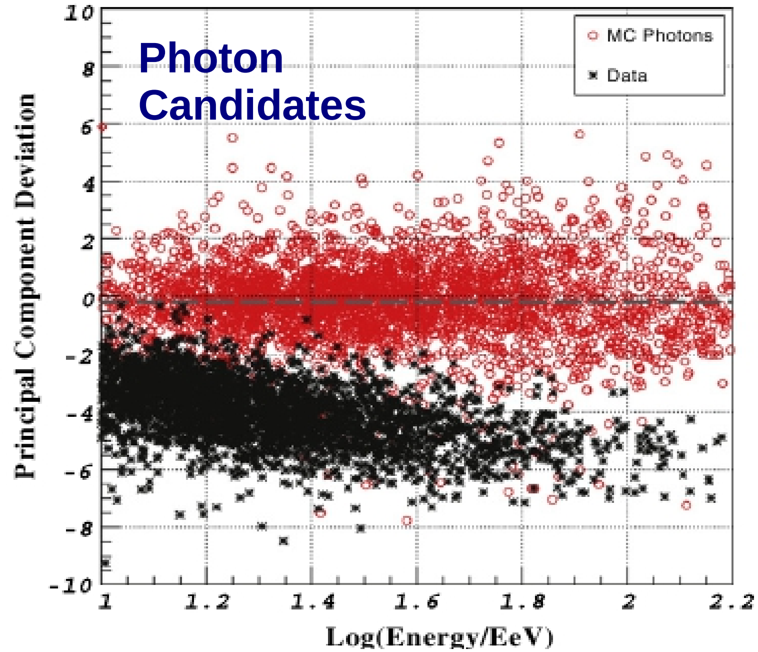

NO photon
candidates

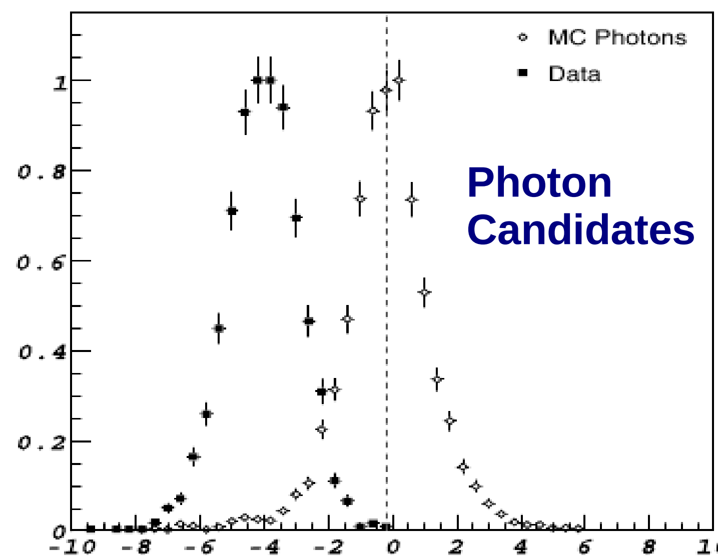

Projection on the principal
component axis

Upper Limit using Hybrid Events

Integral upper limit on the fraction of cosmic ray photons above 1, 2, 3, 5 and 10 EeV.

The results complement previous constraints on top–down models from array data and they reduce systematic uncertainties in the interpretation of shower data.

The basic idea is to combine the measured **X_{max}**, FD observable, with an SD variable, **S_4**.

$$S_b = \sum_i S_i \left(\frac{R_i}{R_{\mathrm{ref}}} \right)^b$$

b=4

S_i : station signal [VEM]

R_i : station distance to the shower axis [m]

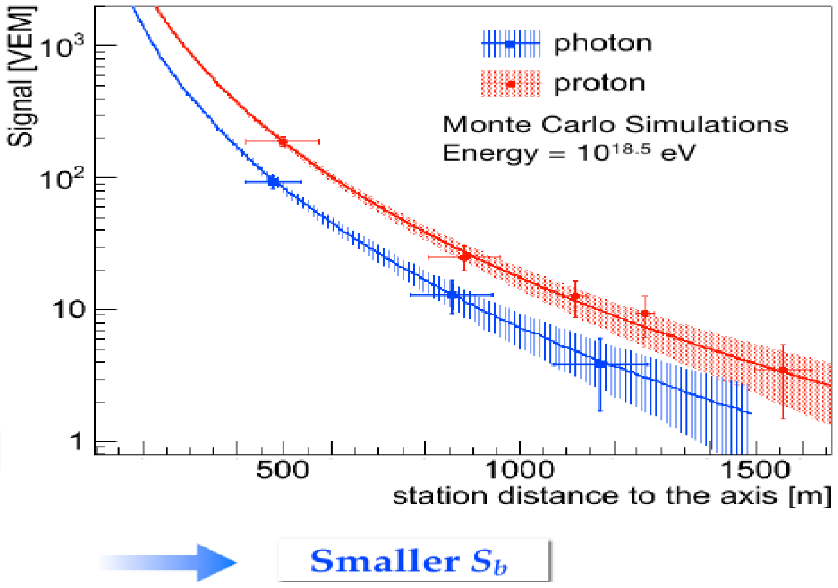

The hybrid data used in this analysis were collected between January 2005 and September 2010.

Discriminant Method

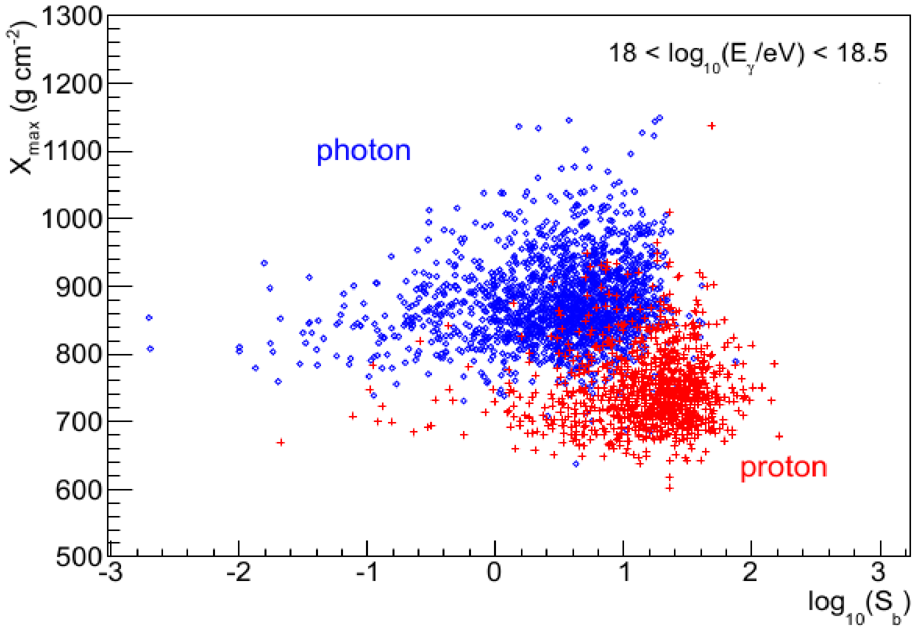

FISHER DISCRIMINANT ANALYSIS

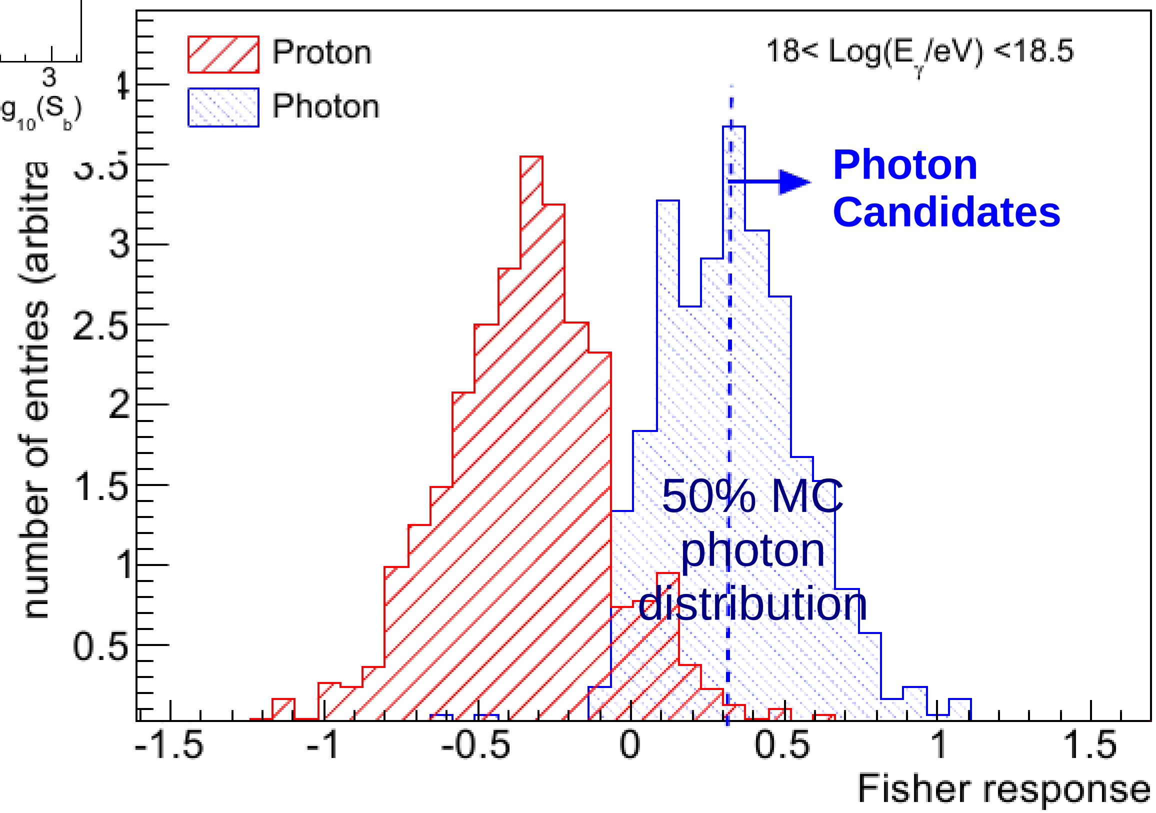

$n_{\gamma\text{-cand,obs}}$ = 6, 0, 0, 0, 0
at E>1, 2, 3, 5, 10

compatible with expected background events

Photon Fraction Upper Limit

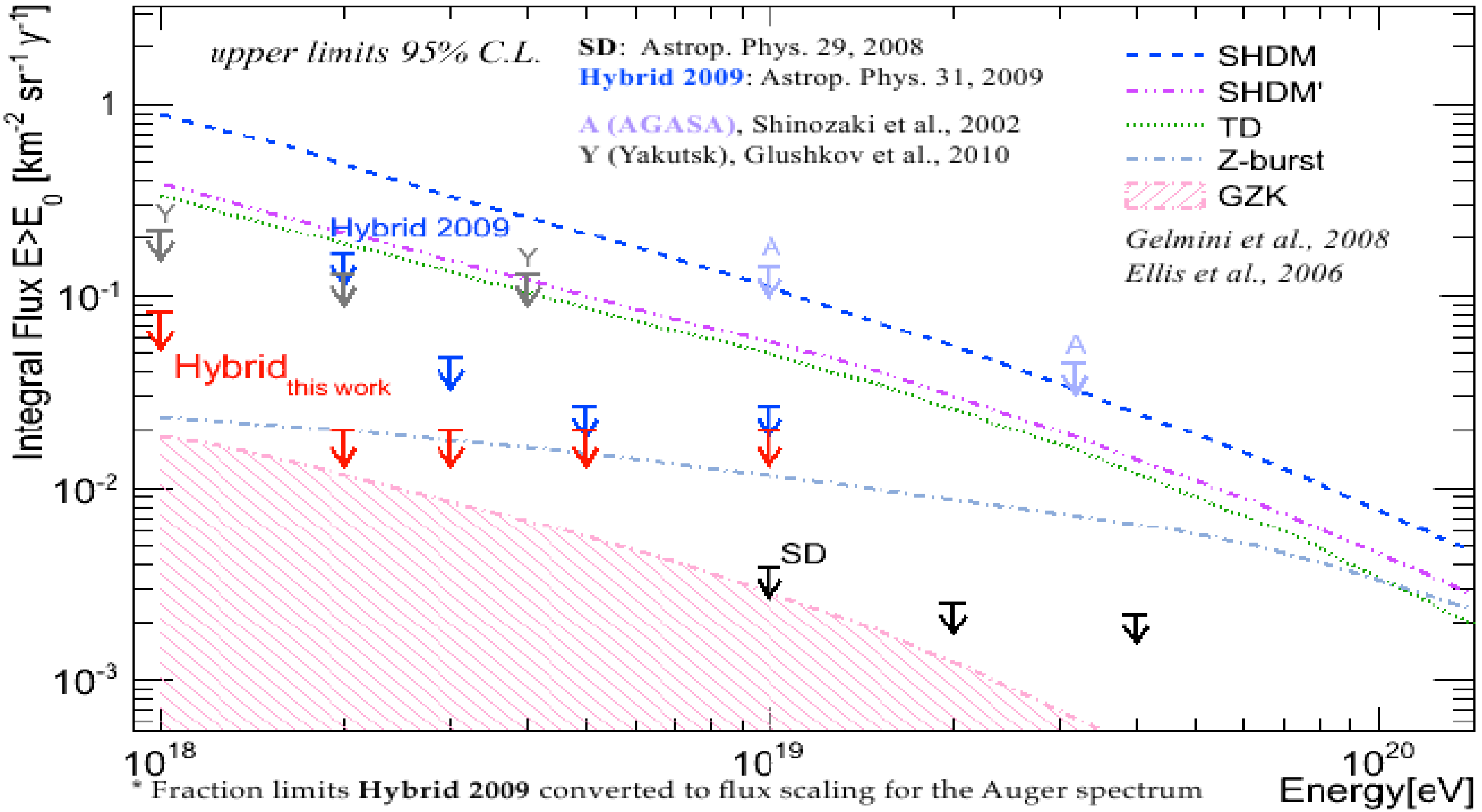

Photon Fraction Upper Limit:
SD: 2.0%, 5.1%, 31% @ E>10, 20, 40 EeV
FD: 0.4%, 0.5%, 1.0%, 2.6%, 8.9% @ E>1, 2, 3, 5, 10 EeV

Directional Upper Limit

A direct way to identify the origins of cosmic rays is to find fluxes of photons coming from discrete sources.

The search in this analysis is sensitive to:

- **Declination band: −85° to +20°**
- **Energy range: $10^{17.3}$ eV to $10^{18.5}$ eV**

The energy range is chosen to account for high event statistics and to avoid additional shower development processes that may introduce a bias at highest energies (pre-shower and LPM).
Showers measured in **hybrid mode** (January 2005-September 2011) are used, so **multiple characteristics of photon-induced air showers** can be exploited by the two detector systems in combination.

ALL EXPOSED CELESTIAL DIRECTIONS (“BLIND” SEARCH)

For a median exposure (the sensitivity depends on the declination), a flux of 0.14 photons km^{-2} yr^{-1} or greater would yield an excess of at least 5σ. This corresponds to an energy flux of 0.25 eV cm^{-2} s^{-1} for a photon flux following a $1/E^2$ spectrum.

Mass Composition-Sensitive

FD Observables

- **Xmax**. In the energy range of this work, the difference between phon and hadron-induced showers is about 100 g cm^{-2};

- **χ^2_{Gr}/dof**. The longitudinal profile can be fitted also with the Greisen function, optimized to describe the longitudinal profile of pure elecromagnetic showers.

- **E_{Gr}/E_{GH}**, where E_{Gr} is the energy obtained by Greisen fit and E_{GH} is that obtained by Gaisser-Hillas fit

SD Observables

- **S_b**, with b=3, optimized for this energetic range;

- **Shape Parameter**, defined as the ratio of the early-arriving to the late-arriving integrated signal as a function of time measured in the water-Cherenkov

$$\mathrm{ShapeP}(r,\theta) = \frac{S_{\mathrm{early}}(r,\theta)}{S_{\mathrm{late}}(r,\theta)}$$

Discriminant Power

MVA Analysis: **Boosted Decision Tree (BDT)** → **separation**, that is defined to be zero for identical signal and background shapes of the output response and it is one for shapes with no overlap.

Observables	*Separation*
all	0.668
No S_b	0.438
No $X_{\max}$	0.599
No $\chi^2_{\mathrm{Gr}}/\mathrm{dof}$	0.662
No $E_{\mathrm{Gr}}/E_{\mathrm{GH}}$	0.664
No ShapeP	0.667

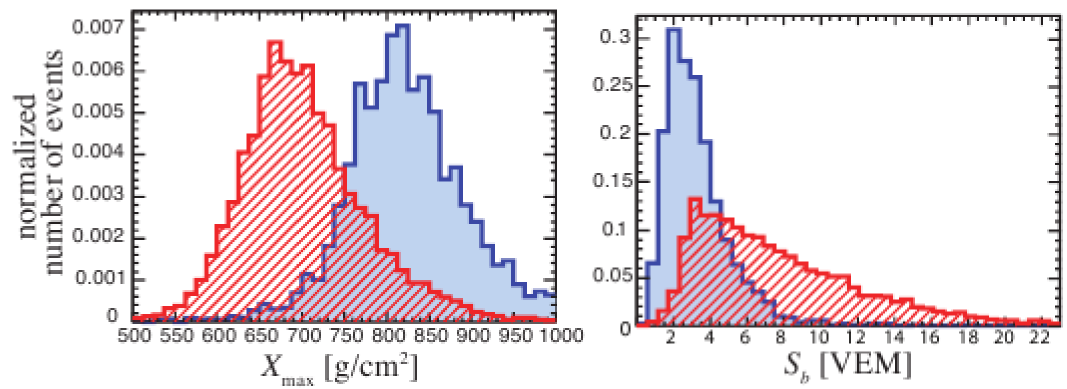

only $X_{\max}$ and S_b → separation=0.645

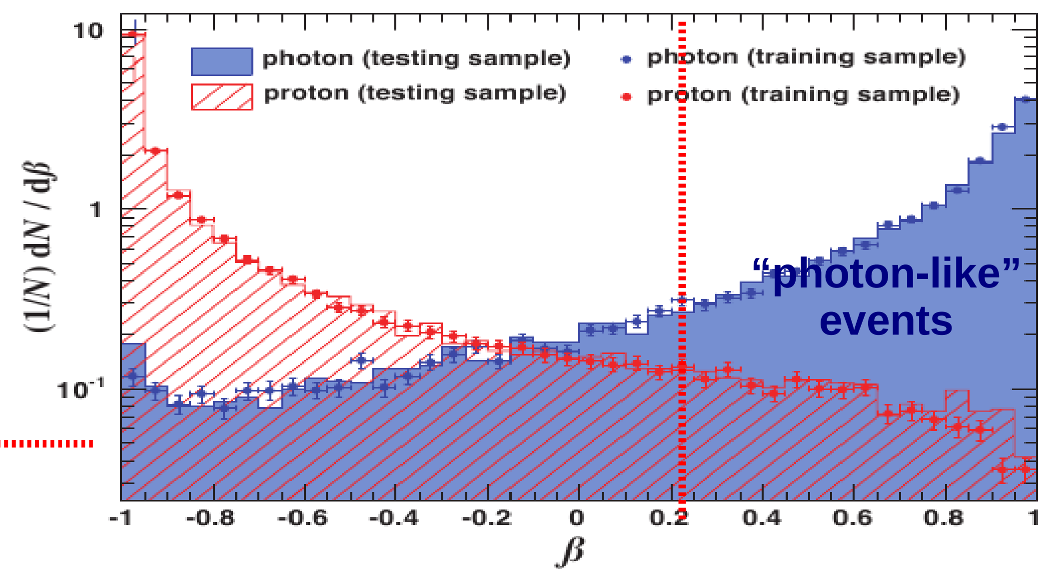

Out response of BDT

Background Expectation

Scrambling technique: use only measured data

1. the arrival directions (in local coordinates) of the events are smeared randomly according to their individual reconstruction uncertainty;
2. N_{data} events are formed by choosing randomly a local coordinate and, independently, a Coordinated Universal Time from the pool of measured directions and times. This procedure is repeated 5000 times.

The mean number of arrival directions within a target is then used as the expected number for that particular sky location.

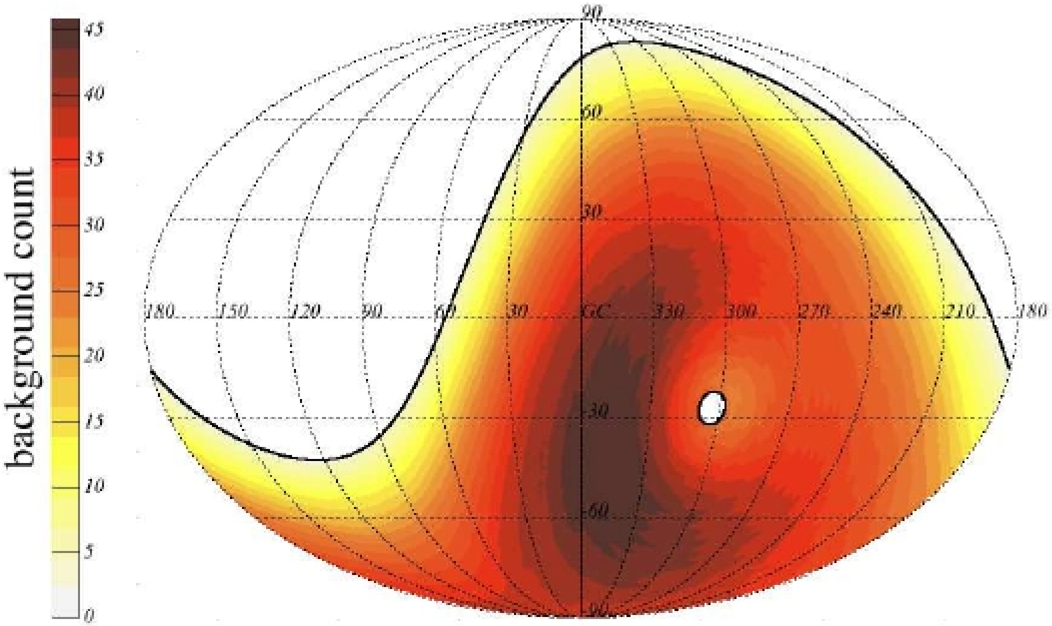

The solid black lines indicate the covered declination range of this analysis.

Blind Search Analysis

The "photon like" sample is composed by the events with **$\beta \geq \beta cut$**.

The β_{cut} is optimized to improve the detection potential of photons, dependent on the expected number of background events $n_b(\alpha,\delta)$, where α and δ are the celestial coordinates.

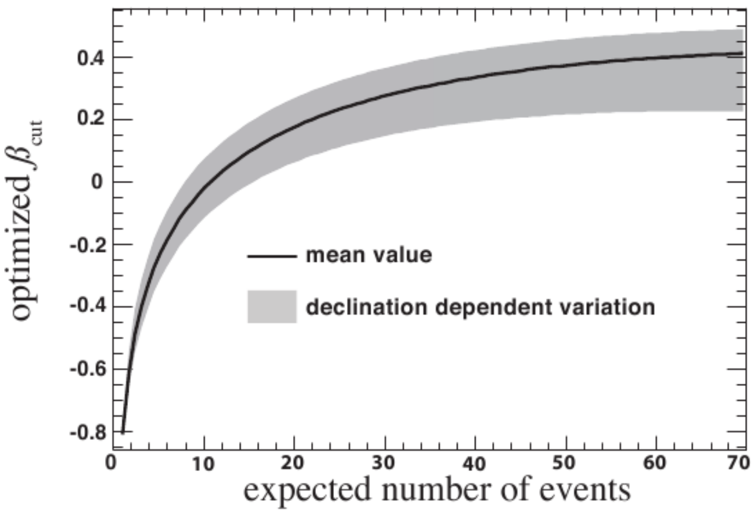

The upper limit on the number of photons n_s from a point source at a given direction is calculated under the assumption that

$n_{data} = n^{\beta}_{b}$, with $n^{\beta}_{b}(\alpha,\delta) = n_b(\alpha,\delta) \cdot \varepsilon^{\beta}_{data}(\delta) \approx 4$

$$P(\leq n^{\beta}_{\mathrm{data}} | n^{\beta}_{b} + n^{\mathrm{Zech}}_{s}) = \alpha_{\mathrm{CL}} \cdot P(\leq n^{\beta}_{\mathrm{data}} | n^{\beta}_{b})$$

Procedure of Zech
α_{CL}=95%

Upper Limit

$$\boxed{f^{\mathrm{UL}} = \frac{n_s^{\mathrm{Zech}}}{n_{\mathrm{inc}} \cdot \mathcal{E}_\beta}}$$

n_{inc}=0.9, expected signal fraction

$$\mathcal{E}_\beta(\alpha, \delta) = \mathcal{E}(\alpha, \delta) \cdot \varepsilon_\gamma^\beta$$

ε^β_γ is the photon efficiency when applying a β_{cut}

$$\mathcal{E}(\alpha, \delta) = \frac{1}{c_E} \int_E \int_T \int_S E^\zeta \; \varepsilon(E, t, \theta, \phi, x, y) \; \mathrm{d}S \; \mathrm{d}t \; \mathrm{d}E$$

$$\zeta = -2$$
$$c_E = \int E^\zeta \; \mathrm{d}E$$

Results

Celestial Map of -log(p)

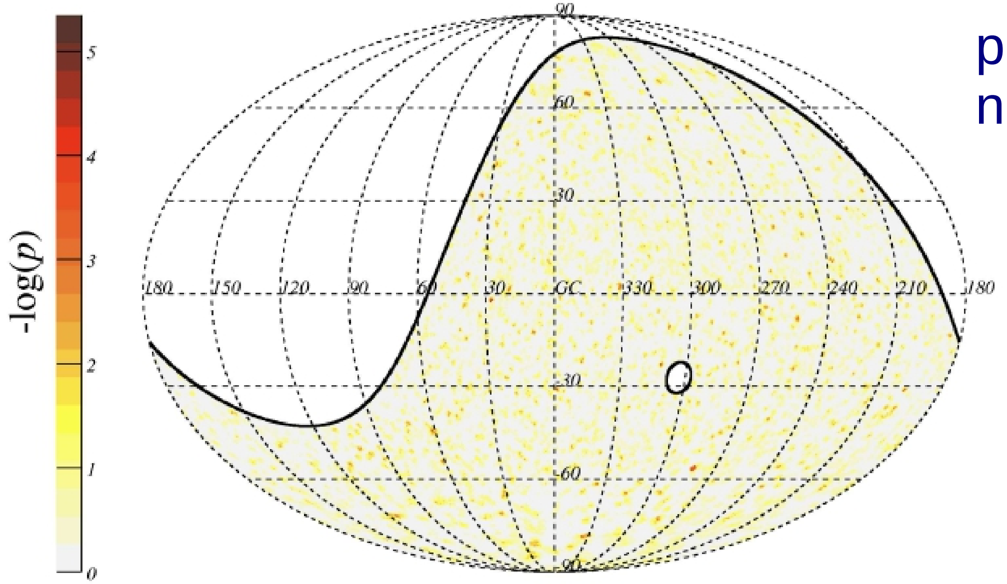

p = Poisson probability of having a number of observed events ≥ expected bkg

$p_{min} = 4.5 \times 10^{-6} \rightarrow p_{chance} = 36\%$

NO SIGNIFICANT EXCESS

Celestial Map of photon flux upper limit

mean value = 0.035 photons $km^{-2}\,yr^{-1}$
(0.14 photons $km^{-2}\,yr^{-1}$)
energy flux = 0.06 eV $cm^{-2}\,s^{-1}$
(0.25 eV $cm^{-2}\,s^{-1}$)

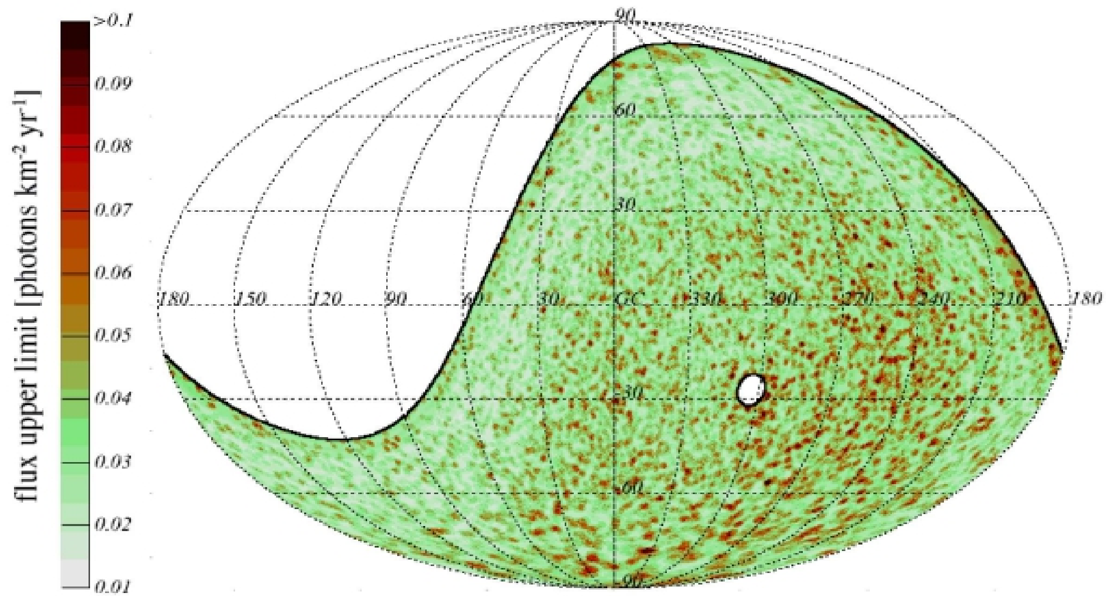

Conclusions

DIFFUSE UPPER LIMITS

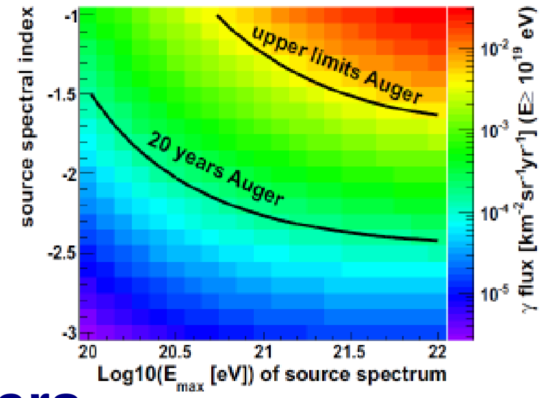

- **No photon events observed;**
- **“Top-down” model disfavoured**;
- **GZK photons could be observed in the next years**

The idea is to enhanced sensitivity with new analysis, upgraded detector, accumulated exposure

DIRECTIONAL UPPER LIMITS

- **No photon point source has been detected;**

It is possible that some genuine photon fluxes are responsible for some of the low p-values. If so, additional exposure should increase the significance of those excesses.

TARGETED SEARCHES ARE ONGOING

Backup

Photons Propagation

Photon-initiated cascades are almost purely elecromagnetic ones. Production of muon pairs is suppressed by $(me\ /m\mu\ )^2$. The **cross-section for photonuclear interactions** which mainly transfer energy to secondary hadrons (and these subsequently to muons), is expected to be ∼10 mb at 10^{19} eV and thus more than **two orders of magnitude below σ_{BH}** (which can be also reduced by the LPM effect).

For UHE proton: depths of shower maxima differ by **30−40 g cm^{-2} between SIBYLL and QGSJET**.

For UHE photons: 5 g cm^{-2}

Preshower Effect

Contrary to nuclear primaries, $\sim 10^{20}$ eV photons can convert in the geomagnetic field to an e± pair which then emits synchrotron photons. Instead of a single UHE photon, a bunch of lower-energy electromagnetic particles, called "preshower", enters the atmosphere with important consequences for the shower development. The local differential probability of photon conversion as well as the probability distribution of synchrotron photons emitted by the electrons, depend on the parameter

$$\chi = \frac{E}{mc^2}\frac{B_\perp}{B_\mathrm{c}} \ , \quad B_\mathrm{c} \sim 4.414 \times 10^{13}\ \mathrm{G}$$

where E is the energy of the parent particle (photon or electron), m the electron mass, Bc a constant, and $B_\perp$ is the local magnetic field component transverse to the direction of the particle's motion. The probability Pconv of a photon to convert in the Earth's magnetic field results from an integration along the particle trajectory; for Pconv $\rightarrow$ 1, photons would almost surely undergo geomagnetic cascading. Non-negligible probabilities (Pconv $\sim$ 10%) are usually obtained for photon with energies above **2–4 × 10^{19} eV** depending on the site.
The preshower effect reduces the average Xmax and its event-by-event fluctuations.

LPM Effect

In a medium, the Bethe-Heitler cross-section for pair production by photons ($\sigma_{BH} \approx 0.51$ b in air) can be reduced due to destructive interference from several scattering centers. This is called LPM (Landau, Pomeranchuk, Migdal) effect. With

$$\kappa = \frac{E_\gamma E_{LPM}}{E_e(E_\gamma - E_e)}, \quad E_{\mathrm{LPM}} = \frac{m^2 c^3 \alpha X_0}{4\pi\hbar\rho} \approx (7.7\ \mathrm{TeV/cm}) \times \frac{X_0}{\rho}$$

the reduced cross-section σ_{LPM} can for $\kappa<1$ be approximated by $\sigma_{LPM} = \sigma_{BH}\mathrm{sqrt}(\kappa) \propto (\rho E_\gamma)^{-1/2}$, with photon energy E_γ, electron energy E_e, radiation length $X_0 \sim 37$ g cm^{-2} in air, density ρ of the medium, and electron mass m.

E_{LPM} ~ 2.8 × 10^{17} eV at 300 m a.s.l. and **~ 10^{19} eV in the upper atmosphere**.

The LPM effect increases the average Xmax and its event-by-event fluctuations.

“Top-Down” Models

The cosmic ray primaries are the result of decay of massive particles originating from high energy processes in the early Universe.

Z-burst: ultra-high energy neutrinos coming from remote sources annihilate at the Z-resonance with relic background neutrinos. The Z bosons then decay, producing secondary protons, neutrinos and photons. The Z-resonance, which acts as a new cutoff, occurs when the energy of the incoming ν is $E_{res} = M_Z / 2m_\nu = 4 \times 10^{21}$ eV.

Topological defects (TD): monopoles, cosmic strings, etc. (TD) produce GUT-scale mass particles, which in turn decay into quarks, leptons etc.
The quarks hadronize and some leptons decay resulting in a large cascade of photons, neutrinos, light leptons and a smaller amount of nucleons.
The mass scale of the parent particles provides the maximum energy of the UHECR (new cutoff at energies above 10^{20} eV).

Super Heavy Dark Matter (SHDM): super heavy metastable particles are produced in early Universe, and they remain at present. They may decay or annihilate into the observed UHECR. The spectra of the decay or annihilation products are essentially determined by the physics of QCD fragmentation and this implies photon domination of the flux at the highest energies.

SD Upper Limits (Selection)

The criteria to select well reconstructed events are:

- the station with the largest signal is surrounded by six active stations;
- ≥ 5 stations used in the fitting of the lateral distribution function out of which ≥ 4 stations have a non-saturated signal of ≥ 10 VEM;
- reduced $\chi^2 < 10 \rightarrow$ radius of curvature;

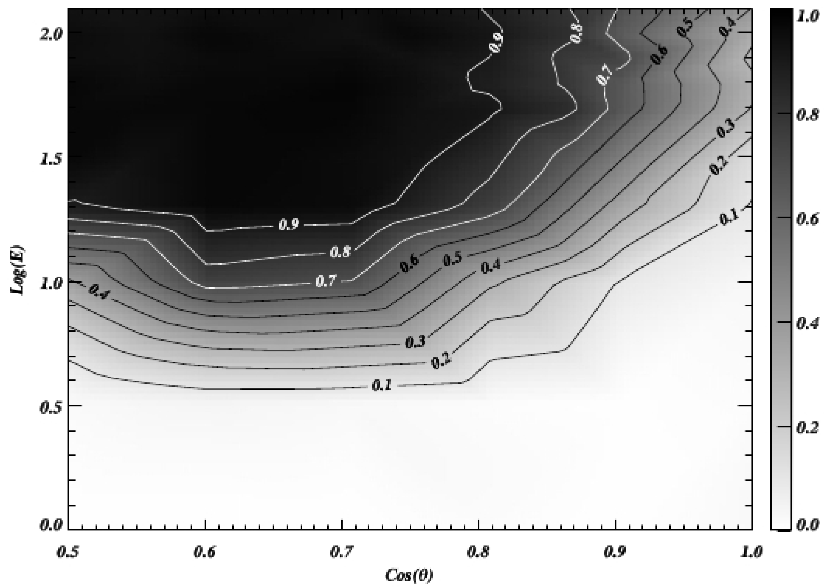

- primary energies ≥ 10 EeV;
- primary zenith angles of 30–60°.

near-vertical photons can also fail the station multiplicity cut due to their deep development

SD Upper Limits

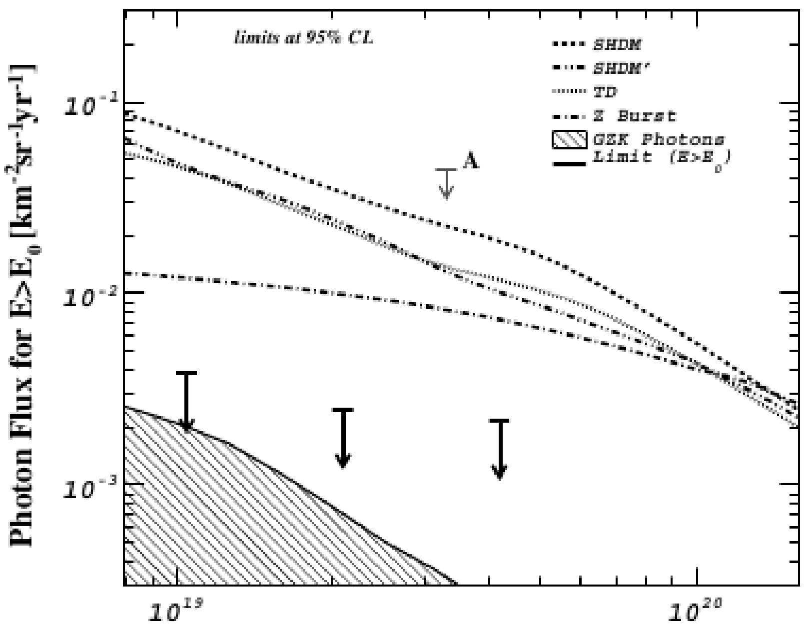

$$\Phi_{\mathrm{CL}}(E > E_{\min}) = \frac{\mathcal{N}_{\gamma}^{\mathrm{CL}}(E_{\gamma} > E_{\min}) \times \frac{1}{f} \times \frac{1}{\varepsilon}}{0.95A}$$

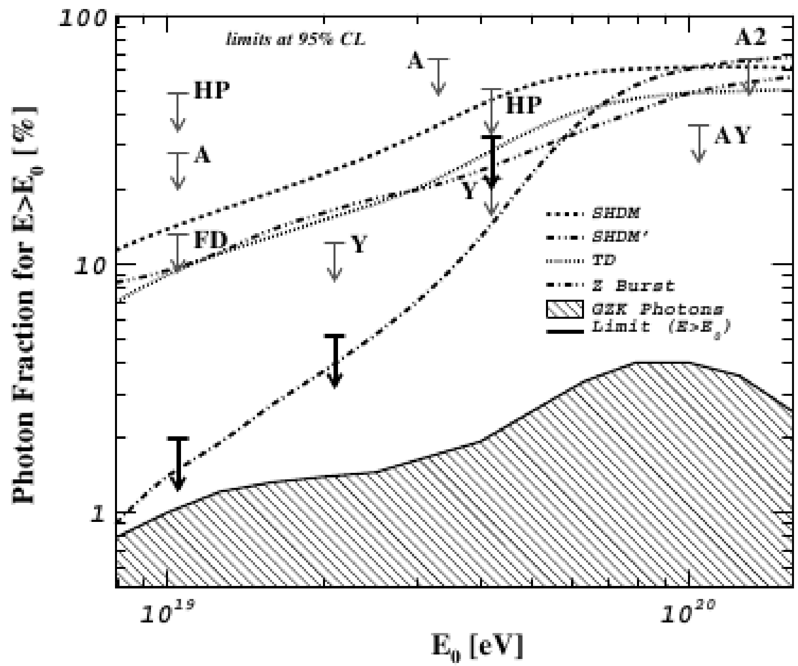

$$\mathcal{F}_{\mathrm{CL}}(E > E_{\min}) = \frac{\mathcal{N}_{\gamma}^{\mathrm{CL}}(E_{\gamma} > E_{\min}) \times \frac{1}{f} \times \frac{1}{\varepsilon}}{N_{\gamma}(E_{\gamma} > E_{\min}) + N_{\text{non-}\gamma}(E_{\text{non-}\gamma} > E_{\min})}$$

$E_{\min}$	$N(E_{\gamma} > E_{\min})$	N_{γ}	$\mathcal{N}_{\gamma}^{0.95}$	$N_{\text{non-}\gamma}$	ε	$\Phi_{0.95}$	$\mathcal{F}_{0.95}$ (%)
10	2761	0	3.0	570	0.53	3.8×10^{-3}	2.0
20	1329	0	3.0	145	0.81	2.5×10^{-3}	5.1
40	372	0	3.0	21	0.92	2.2×10^{-3}	31

SD Upper Limit Systematics

Changing the power law index from -2 to -1.7, -2.5 and -3., the number of events which are photon candidates is unchanged (along with the number of non-photon candidate events), but the correction for the photon efficiency changes. Specifically, for a steeper input spectrum (increased fraction of lower-energy photons), the efficiency decreases. For 10 EeV threshold energy, limits change from (3.8 → 5.5) x 10-3 km-2sr-1yr-1 for the flux and from (2.0 → 2.9)% for the fraction. The differences get smaller with increased threshold energy.

The photonuclear cross-section used in the simulation is based on the Particle Data Group (PDG) extrapolation. For an increased cross-section, more energy would be transferred to the hadron (and muon) component which could diminish the separation power between data and primary photons. From simulations with modified cross-sections it was verified that this leads to a negligible variation of the average values of the discriminating variables used in the current analysis.

Selection Cuts Hybrid Events

For FD:

- a reduced $\chi 2$ of the longitudinal profile fit to the Gaisser-Hillas function smaller than 2.5;
- a $\chi 2$ of a linear fit to the longitudinal profile exceeding the Gaisser-Hillas fit $\chi 2$ by at least a factor of 1.1;
- the Xmax observed within the field of view of the telescopes;
- the Cherenkov light contamination smaller than 50%;
- the uncertainty of the reconstructed energy less than 20%.

Only time periods with the sky not obscured by clouds and with a reliable measurement of the vertical optical depth of aerosols, are selected.

For SD:

- we require at least 4 active stations within 2 km from the hybrid reconstructed axis. This prevents an underestimation of Sb due to missing or temporarily inefficient detectors.assumption.

Hybrid Photon Candidates

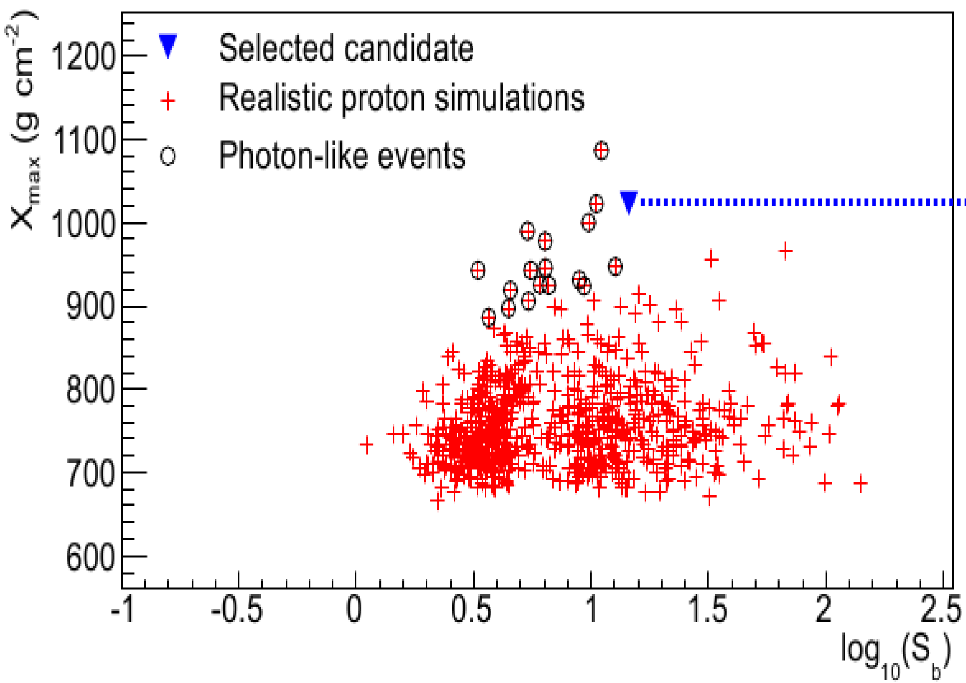

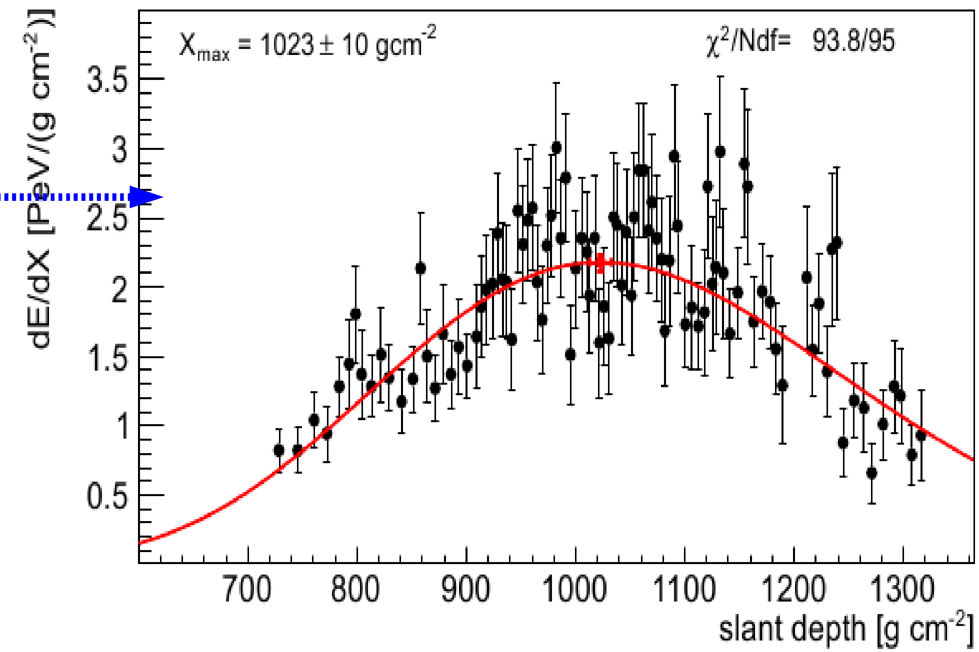

$n_{\gamma\text{-cand,obs}}$ = 6, 0, 0, 0, 0
at E>1, 2, 3, 5, 10
compatible with expected background events

$$\Phi_{\gamma}^{95CL} = \frac{N_{\gamma}^{95CL}(E_{\gamma} > E_0)}{\mathcal{E}_{\gamma,\mathrm{min}}}$$

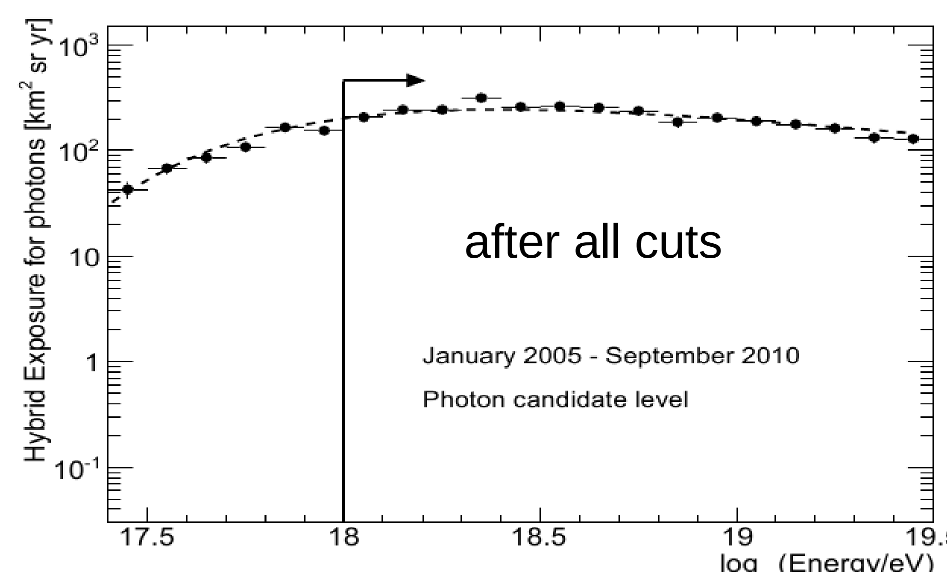

Hybrid Upper Limit Systematics

- Increasing (reducing) all Xmax values by the uncertainty ΔXmax = 13 g cm^{-2} changes the number of photon candidates above 1 EeV by +1 (-2) not affecting the higher energies. As a consequence, this leads to an increase of ∼10% (decrease of ∼ 25%) of the first point of the upper limits.

- The uncertainty on the shower geometry determination corresponds to ΔSb∼5%, changing the number of photon candidates by ±0 (+1) above 1 EeV.

- The overall uncertainty on the hybrid exposure calculation for photons is about 5%. It includes the uncertainty due to on-time calculation (∼4%), input spectra for Monte Carlo simulations and dependence of the trigger efficiency on the fluorescence yield model (∼2%).

- Another source of systematic uncertainties is the energy scale which has been estimated to be about 22% . An increase (reduction) of the energy scale, keeping the energy thresholds E0 fixed, would change the upper limits by +14% (-54%) above 1 EeV and by +6% (-7%) above 2, 3, 5 and 10 EeV.

Shape Parameter

Defined as the ratio of the early-arriving to the late-arriving integrated signal as a function of time measured in the water-Cherenkov

$$\mathrm{ShapeP}(r,\theta) = \frac{S_{\mathrm{early}}(r,\theta)}{S_{\mathrm{late}}(r,\theta)}$$

The early signal S_{early} is defined as the integrated signal over time bins less than a scaled time tscaled ≤ 0.6 µs, beginning from the signal start moment. The scaled time varies for different inclination angles θ and distances r to the shower axis and can be expressed as:

$$t_i^{\mathrm{scaled}}(r,\theta) = t_i \cdot \frac{r_0}{r} \cdot \frac{1}{c_1 + c_2 \cdot \cos(\theta)}$$

where t_i is the real time of bin i and r_0 = 1000 m is a reference distance. c1 = −0.6 and c2 = 1.9 are scaling parameters to average traces over different inclination angles. Correspondingly, the late signal S_{late} is the integrated signal over time bins later than t_{scaled} > 0.6 µs, until signal end.

Directional Upper Limit Systematics

- Systematic uncertainty of the Auger energy scale:
  +14% → mean upper limit +8%
  -14% → mean upper limit -9%
  (change in particular photon exposure)

- Changing high energy hadronic model: QGSJET-01 → EPOS-LHC
  → -9%

- Spectral index: -2 → -1.5
  -34%

  -2 → -2.5
  +51%

  The changing on the flux are related to the changing in the directional photon exposure

Directional Upper Limit Observations

The energy flux in TeV gamma rays exceeds 1 eV cm^{-2} s^{-1} for some Galactic sources with a differential spectral index of E^{-2} . A source with a differential spectral index of E^{-2} puts out equal energy in each decade, resulting in an expected energy flux of 1 eV cm^{-2} s^{-1} in the EeV decade. No energy flux that strong in EeV photons is observed from any target direction, including directions of TeV sources such as Centaurus A or the Galactic center region.

Results from the present study complement the blind search for fluxes of neutrons above 1 EeV previously published by the Auger Collaboration. No detectable flux was found in that search, and upper limits were derived for all directions south of declination $+20^\circ$. Neutrons and photons arise from the same types of pion-producing interactions.

Directional Upper Limit Observations (1)

The absence of detectable point sources of EeV neutral particles does not mean that the sources of EeV rays are extragalactic:

- It might be that EeV cosmic rays are produced by transient sources such as gamma ray bursts or supernovae. The Auger Observatory has been collecting data only since 2004. It is quite possible that it has not been exposed to neutral particles emanating from any burst of cosmic-ray production.

- Alternatively, it is conceivable that there are continuous sources in the Galaxy which emit in jets and are relatively few in number, and if so none of those jets are directed toward Earth.

- Another possibility is that the EeV protons originate in sources with much lower optical depth for escaping than is typical of the known TeV sources. The production of neutrons and photons at the source could be too meager to make a detectable flux at Earth.